

## Effect of shock pressure and plastic strain on chemical reactions in Nb–Si and Mo–Si systems

M.A. Meyers<sup>a,b</sup>, S.S. Batsanov<sup>b,1</sup>, S.M. Gavrilkin<sup>1</sup>, H.C. Chen<sup>b</sup>, J.C. LaSalvia<sup>a</sup>,  
F.D.S. Marquis<sup>a,2</sup>

<sup>a</sup>*Institute for Mechanics and Materials, University of California, San Diego, La Jolla, CA 92093, USA*

<sup>b</sup>*Department of Applied Mechanics and Engineering Sciences, University of California, San Diego, La Jolla, CA 92093, USA*

Received 21 October 1994; in revised form 19 December 1994

### Abstract

Nb–Si and Mo–Si elemental powder mixtures contained within cylindrical capsules were subjected to co-axial shock-wave loading at varying pressures (2.8–70 GPa). Shock-induced or shock-assisted chemical reactions were observed in these powder mixtures along the capsule axis. Three concentric regions with the capsules were observed: (1) fully reacted (Mach stem region); (2) partially reacted; and (3) unreacted. These results confirm the Krueger–Vreeland concept of threshold energy for shock-induced chemical reactions. Analysis of partially reacted regions enabled the identification of the reaction micromechanisms in accordance with the model proposed by Meyers, Yu and Vecchio (*Acta Metall. Mater.*, 42 (1994) 715). Asymmetric shock-wave loading experiments on the above powder mixtures were also conducted. Significant macroscopic plastic deformation (i.e.  $\epsilon \cong 0.2$ –0.5) along with consolidation were achieved by modifying the explosive loading configuration. Because of the asymmetric loading, regions of shear localization were produced. These regions were also characterized by the onset of the chemical reaction resulting from the local thermal excursion due to both the frictional dissipation of kinetic energy and plastic deformation. The results obtained in this investigation confirm the earlier hypothesis that the shock energy dissipated by plastic deformation does play an important role in the initiation of the chemical reaction. It is proposed that the Krueger–Vreeland threshold energy be modified to take into account the plastic deformation energy.

**Keywords:** Shock pressure; Plastic strain; Nb–Si; Mo–Si

### 1. Introduction

Shock waves have been known to initiate chemical reactions in solids for a long time. The detonation of explosives is the classic example of this phenomenon. In more recent years, displacive phase transformations, decompositions, and chemical reactions have been induced by the propagation of shock waves. The first report of chemical changes occurring due to the application of shock compression is due to Ryabinin [1]. At the same time, Bancroft et al. [2] described the alpha-epsilon phase transition undergone by iron at 13 GPa

shock pressure. The synthesis of diamond from graphite, or directly from the detonation products of explosives, is a direct application of this concept. De Carli and Jamieson [3,4] in the early 1960s were the pioneers in this field, having demonstrated that diamond particles (<10 mm) could be produced from graphite. The early work by Nomura [5,6] and Horiguchi [7] in Japan, Adadurov et al. [8] and Batsanov and Deribas [9] and co-workers in Russia demonstrated that new compounds can be synthesized from powder mixtures through the propagation of a shock wave. A number of studies ensued, leading to the synthesis of numerous ceramic and intermetallic compounds via shock-induced chemical reactions between powders: silicides, aluminides, carbides, and other compounds. In the U.S., Graham [10], Horie [11–13] and co-workers played a key role in shock synthesis. Lange and Ahrens [14] studied the decomposition of  $\text{CaCO}_3$

<sup>1</sup> Permanent address: Center for High Dynamic Pressures, National Institute of Standards, Mendeleev, Moscow Region, Russia.

<sup>2</sup> Permanent address: Department of Metallurgical Engineering, South Dakota School of Mines and Technology, Rapid City, SD 57701, USA.

into  $\text{CO}_2$  and  $\text{CaO}$  induced by shock waves; this study has important geological implications. Three books were recently published with strong emphasis on shock-induced reactions: Graham [15], Horie and Sawaoka [16], and Batsanov [17]. Additionally, the monograph by Thadhani [18] is a comprehensive review. In 1984, the National Materials Advisory Board concluded a study on shock compression chemistry (Duvall [19]).

Batsanov and co-workers [20,21] reported anomalies in the pressure–volume Hugoniot curves produced by reactions. The pressure–volume curve for a reacting mixture shifted to the right, in analogy with explosives. This shift leads to alterations in pressure, particle velocity, and shock velocity, since a new thermodynamic state is accessed. Similar results were predicted by Boslough [22] and Yu and Meyers [23]; they simply added the energy of reaction,  $E_R$ , to the conservation-of-energy equation:

$$E - E_{00} = \frac{1}{2}(P + P_0)(V_{00} - V) + E_R \quad (1)$$

There are essentially two schools of thought regarding the onset of shock-induced chemical reactions: solid–solid vs. solid–liquid reactions. Graham [15] and Batsanov [17] provide substantial evidence in favor of the former mechanism whereas Krueger et al. [24–26], Vecchio et al. [27], and Meyers et al. [28] obtained results that substantiate a solid–liquid reaction.

The seminal paper by Dremin and Breusov [29] addresses the issue of shear deformation in shock processing to a considerable detail. The early work by Bridgman [30–33] showed that shear deformation, superimposed on hydrostatic pressure, resulted in chemical reactions. Vereshchagin and co-workers [34] confirmed the enhanced reactivity produced by shear deformation, and Teller [35] supported the contention that reaction rates could be accelerated by shear deformation superimposed on high pressures. Enikolopyan and co-workers [36–39] used a Bridgman cell and subjected a large number of chemical substances and mixtures to pressures, and simultaneous pressure and shear deformation. Their extensive studies confirmed the earlier findings of explosive reactions by Bridgman.

It was serendipitously discovered that plastic deformation, in addition to that normally occurring in the shock compression of powders, can have a significant effect on shock-induced chemical reactions. Shock densification experiments conducted on powder mixtures containing Mo and Si, or Nb and Si, revealed the formation of localized reaction regions in narrow bands produced by shear localization (Yu and Meyers [40]). Experiments also showed that plastic deformation influenced the reaction between elemental Nb and Si powders (Yu et al. [41]). Under shock (pressure) conditions which would not ordinarily result in reaction, localized regions in which the powder mixture had been intensely

deformed plastically underwent chemical reaction. The powder mixture was extruded into the threaded regions by pressure differentials in capsule. The powder being deformed in the threaded regions reacted, because of the high local plastic strains. Nesterenko et al. [42] carried out controlled shear experiments, in the absence of shock compression, and demonstrated that reaction could take place.

The work whose results are presented herewith had two-fold objectives: (a) to confirm the concept of a threshold energy, below which no reaction is initiated; (b) to establish, in a controlled manner, whether plastic deformation can initiate reactions at shock pressures below the threshold level. A cylindrical shock densifying geometry was chosen because the Mach stem formation, along the central axis, produces two clearly distinguishable pressure levels. The pressure in the Mach stem is approximately seven times that in the periphery. The cylindrical geometry was modified by the application of an asymmetrical explosive charge which generates significant plastic deformation in addition to shock compression.

## 2. Experimental procedures

Elemental Nb, Mo, and Si were obtained from CERAC in the form of powders of controlled size. All powders had a size less than 325 mesh (44  $\mu\text{m}$ ). The powders were mixed in the stoichiometric proportions  $\text{NbSi}_2$  and  $\text{MoSi}_2$  and were loaded into tubular steel capsules. The powder mixture had an initial density of 70% of its theoretical value (30% porosity). These capsules, with external diameters of 14 mm and lengths of 70–80 mm, had walls with thicknesses of 2 mm (lower pressure experiments) and 3 mm (higher pressure experiments). The capsules were placed in explosive containers as shown in Fig. 1. The explosive was initiated at the top and the detonation wave traveled downwards, generating high pressures in the capsules. Details of the experimental setup are provided by Batsanov [17]. Three explosives were used with the characteristics given in Table 1: a high ( $\Pi\text{BB-4}$ ), a medium (RDX), and a low detonation velocity explosive (Ammonit). The Russian  $\Pi\text{BB-4}$  explosive is a plastic RDX-TNT mixture; RDX is used in powder form; the low detonation explosive, Ammonit, is an (ammonium nitrate)–(aromatic nitro compound) mixture. These explosives are intended at generating three pressure levels within the capsule. The cylindrical capsule geometry generates a pattern of converging shock waves in the powders, which is well described by Batsanov [17], Prummer [43], and Meyers and Wang [44], among others. The calculated pressures generated by the three explosives are given in Table 1 and are 10.6 GPa ( $\Pi\text{BB-4}$ ), 6 GPa (RDX) and 2.8 GPa (Ammonit).

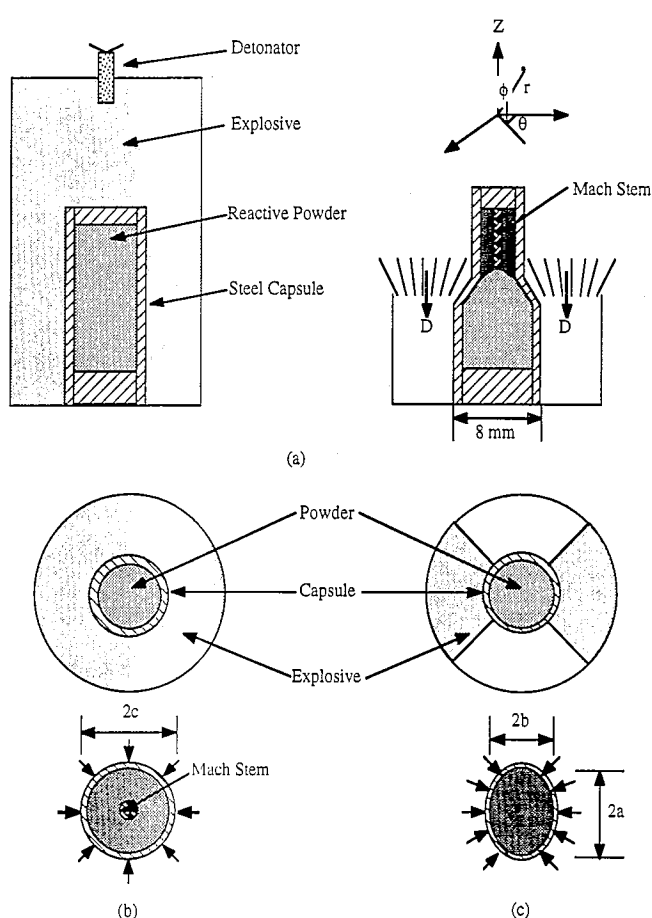


Fig. 1. Experimental configurations used for creating shock-induced chemical reactions: (a) symmetrical explosive configuration with Mach stem generation (longitudinal sections); (b) symmetrical loading configuration (cross-sections); and (c) asymmetrical loading configuration (cross-sections).

The calculational procedure is described by Batsanov [17] and Meyers [40], among others. It should be noted that these are only estimated values, and that the pressure is calculated neglecting the effect of the steel

Table 1  
Explosives used, their principal characteristics, and pressures generated

Property	Explosive		
	PIBB-4	RDX	Ammonit
Density ( $\text{g cm}^{-3}$ )	1.45	1	1.1
Det. Vel. ( $\text{km s}^{-1}$ )	7.4	6.2	4.4
Isentropic gas constant ( $\gamma$ )	2.97	2.66	2.87
Pressure (GPa)			
Nb + 2Si (70%)			
Periphery	10.3	5.9	2.7
Mach stem	68.9	43.8	18.6
Pressure (GPa)			
Mo + 2Si (70%)			
Periphery	10.5	6.0	2.8
Mach stem	70.4	44.9	19.3

capsule. The actual pressures are probably somewhat lower. It is also important to note that the pressures are not constant throughout the cylinder cross-section. More accurate predictions, using hydrocode computation, have been developed by Reaugh [45]. Along the capsule axis, the convergent waves reinforce themselves and form a region in which the shock front is parallel to the propagation direction of detonation. This is the classical Mach stem, first observed in the propagation of shock waves in fluids. In the Mach stem, the shock-wave velocity,  $U_s$ , equals the detonation velocity,  $D$ . From this equality, the pressure can be established. The pressures in the Mach stem, listed in Table 1, are approximately seven times the pressure in the periphery. Only the PIBB-4 explosive generated a pressure sufficiently high for Mach stem formation, and this Mach stem, shown schematically in Fig. 1, is clearly visible by observation of the polished cross-sections of the recovered specimens.

The use of an asymmetrical explosive loading, shown in Fig. 1(b), leads to a distortion of the capsule shape as well as the reduction in overall diameter due to densification. The macroscopic strains imparted by the three loading conditions can be calculated in the reference system defined in Fig. 1(a). The length of the capsules remains unchanged, and therefore  $\epsilon_z = 0$ . The macroscopic plastic strain corresponding to the porosity collapse is:

$$(1 + \epsilon_r)(1 + \epsilon_\theta)(1 + \epsilon_z) = 0.7$$

$$\epsilon_r = \epsilon_\theta = -0.16 \quad (2)$$

The effective strain is  $\epsilon_{\text{eff}} = 0.2$ . In the asymmetric capsules, an additional component of strain is present. It can be calculated from the dimensions  $a$  and  $b$  in Fig. 1(c). Assuming an elliptical distortion, the strain is given by:

$$\epsilon_a = \ln\left(\frac{a}{c}\right)$$

$$\epsilon_b = \ln\left(\frac{b}{c}\right)$$

$$\epsilon_a = -\epsilon_b = 0.55 \quad (3)$$

The corresponding effective strain is  $\epsilon_{\text{eff}} = 0.64$ . The specimens were observed by scanning electron microscopy. The backscattering mode in all micrographs was used to differentiate the phases formed; the light phase is Mo or Nb, the dark phase is Si, and grey phases are compounds.

### 3. Results and discussion

The results will be presented and discussed separately for the two experimental configurations, starting with the symmetrical one.

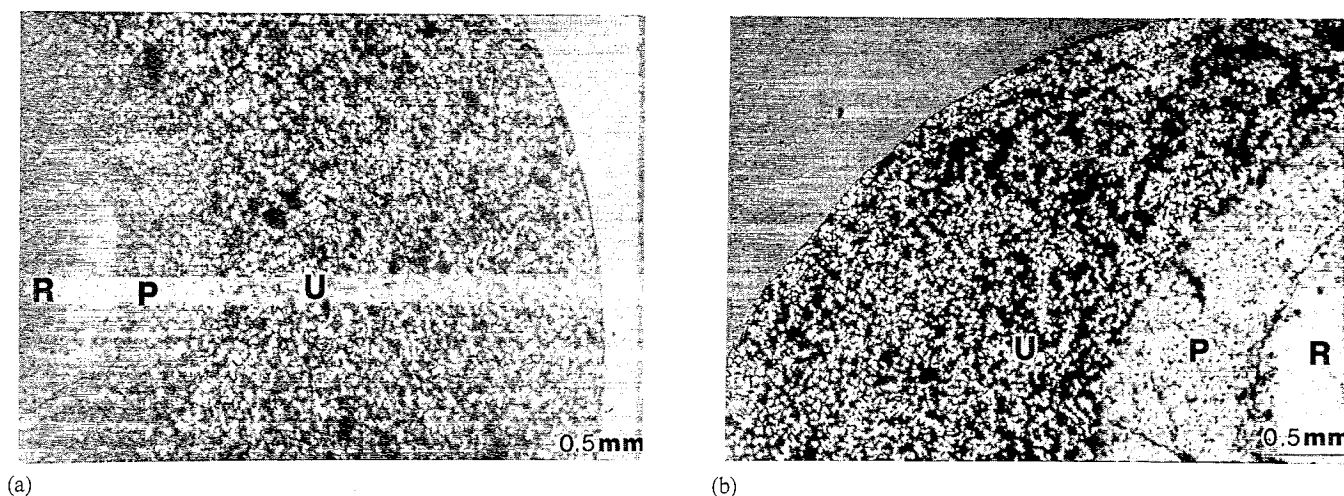


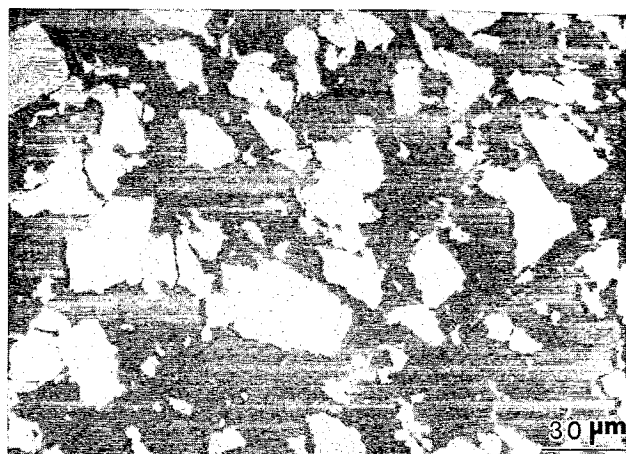
Fig. 2. Low-magnification scanning electron micrographs of cross-sections of (a) Nb-Si and (b) Mo-Si powder mixtures, showing peripheral and Mach stem regions.

### 3.1. Symmetrical configuration

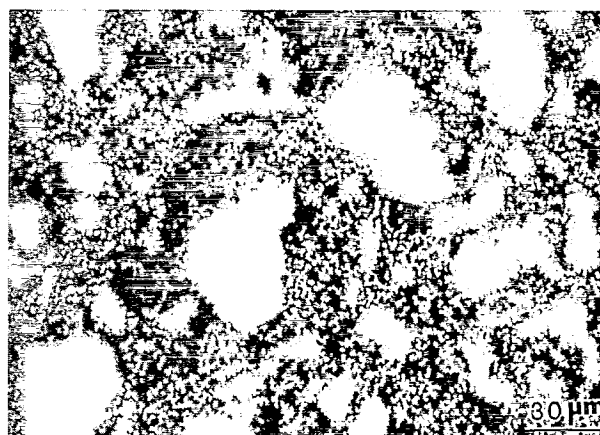
Experiments were conducted using explosive PIBB-4, with a detonation velocity of  $7.4 \text{ km s}^{-1}$ . Both the Mo + 2Si and Nb + 2Si systems exhibited unreacted, partially reacted, and fully reacted regions. Fig. 2 shows a macroscopic view of the cross-sections. These regions are marked U, P, R, respectively. There is a clear boundary between them, and the central Mach stem corresponds to the fully reacted region. The unreacted and partially reacted regions are seen in greater detail in Fig. 3 (Nb + 2Si) and Fig. 4 (Mo + 2Si). The unreacted region corresponds to the periphery of the circular section and was subjected to a calculated pressure of 10 GPa. There is no evidence of Si melting or reaction. Vecchio et al. [27] observed the onset of reaction in shock-compressed Nb + 2Si and Mo + 2Si powder mixtures with the same initial porosity as the present investigation: the onset for reaction was 7–12 GPa. This is consistent with the current results. It is probable that the pressure calculated in Table 1 is an overestimation. The partially reacted region is characterized by the formation of NbSi<sub>2</sub> and MoSi<sub>2</sub> spherules, as observed first by Yu and Meyers [47] and described in detail by Vecchio et al. [27] and Meyers et al. [28]. These spherules have diameters of 0.5–2  $\mu\text{m}$  and are larger in the periphery of Mo particles, as seen in Fig. 4(b). As the Mo particles are consumed, the diameters of the spherules decrease. The gradation of spherule size is seen in the totally consumed particles of Fig. 4(b). Closer to the cylinder axis, a fully reacted region is seen Fig. 5. The presence of profuse spheroidal voids is an indication of complete melting of the reaction products. Two phases are seen for the Nb + 2Si system. These are probably NbSi<sub>2</sub> and Nb<sub>5</sub>Si<sub>3</sub>. Fig. 5(b) shows the boundary between the partially reacted and the fully reacted region for Mo + 2Si. The size of the MoSi<sub>2</sub>

spherules increases gradually, as the Si (dark phase) is consumed. These particles become gradually more faceted. Their maximum size is approximately 10  $\mu\text{m}$ . The right-hand side of Fig. 5(b) shows profuse pores, complete reaction, and the separation of a second lighter phase (and therefore, richer in Nb). Vecchio et al. [27] identified the phase as Mo<sub>5</sub>Si<sub>3</sub>.

The detailed nature of reaction, “frozen in” the partially reacted region, can be seen in Figs. 6 and 7. It is very significant that a sharp interface between (mostly) unreacted and partially reacted regions exists. There has been considerable debate over the time at which the shock-induced chemical reactions occur. From Fig. 6 it is evident that the reaction was triggered by the shock wave, and not by post-shock thermal effects. The physical state of reactants has been analyzed by Vecchio et al. [27] and Meyers et al. [28]. They proposed that silicon melts, whereas niobium (or molybdenum) remains in the solid state. Thadhani [49] recently carried out a systematic analysis of chemical reactions produced by shock compression, classifying them into shock-induced (reaching completion during shock-wave passage) and shock-assisted (occurring primarily after shock compression). From the present results, it is not possible to establish clearly which of these processes is taking place. If thermal (post shock) effects were dominant, one would observe a gradual reduction in the extent of reaction with distance from the interface. Such is clearly not the case; Fig. 7 shows details of the reaction for both the Nb + 2Si and Mo + 2Si cases. The reaction proceeds according to the mechanism described by Meyers et al. [28]. The exothermicity of the reaction is such that the product, NbSi<sub>2</sub>, is formed at a temperature above its melting point. Capillarity effects lead to the formation of spheroids, which minimize the interfacial energy. Fig. 7(a) shows details of the separation of the NbSi<sub>2</sub> layer



(a)

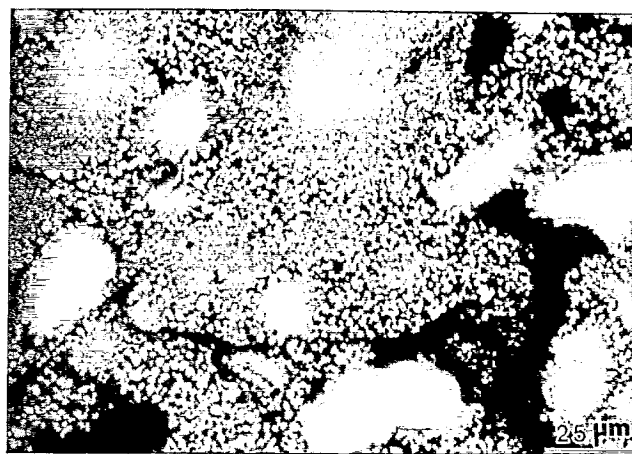


(b)

Fig. 3. (a) Unreacted and (b) partially reacted regions for Nb + 2Si system (symmetric shock compression).

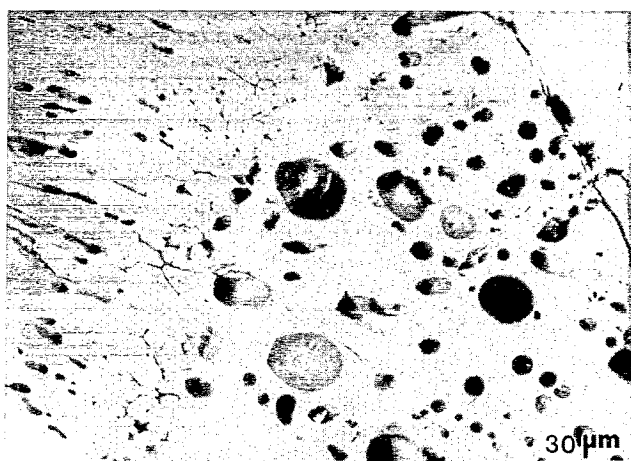


(a)

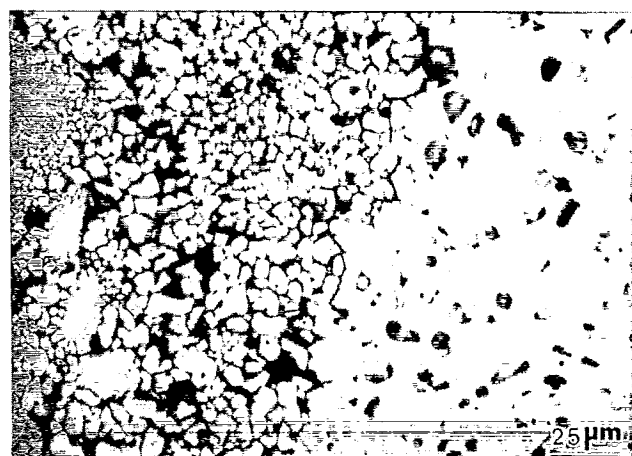


(b)

Fig. 4. (a) Unreacted and (b) partially reacted regions for Mo + 2Si system (symmetric shock compression).



(a)



(b)

Fig. 5. Fully reacted regions from Mach stem from (a) Nb + 2Si system; (b) Mo + 2Si (symmetric shock compression).

from the Nb particles, these regions are marked by arrows. As the NbSi<sub>2</sub> solidifies, stresses are set up which lead to the separation of the spherules from the Nb substrate. The spherules subsequently move into the Si,

which is molten during reaction. The melting points of the three phases are: M.P. Si: 1685 K; M.P. Nb: 2740 K; M.P. NbSi<sub>2</sub>: 2420 K. The same mechanism is seen to operate for MoSi<sub>2</sub>.

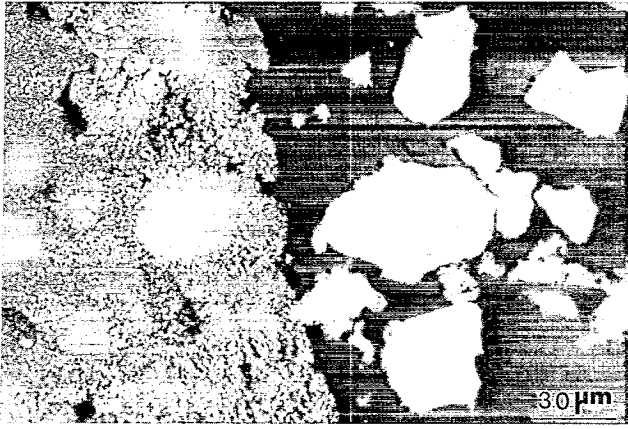


Fig. 6. Interface between peripheral ( $P \approx 10$  GPa) and Mach stem region ( $\approx 30$  GPa) in symmetric shock compression system (Mo + 2Si).

### 3.2. Asymmetrical configurations

Experiments were conducted at two detonation velocities, 4.4 and 6.2 km s<sup>-1</sup>, yielding pressures of approximately 2.8 and 6 GPa (see Table 1). These pressure levels are below the critical level for shock induced chemical reactions, defined by Krueger et al. [25,26] and determined for Nb and Mo silicides by Vecchio et al. [27]. The macroscopic deformation accomplished through asymmetric loading is given in Section 2; the effective strain is 0.64. The deformation energy per unit mass can be estimated from the simple expression:

$$E_d = \frac{\sigma_{\text{eff}} \epsilon_{\text{eff}}}{\rho} \quad (4)$$

where  $\sigma_{\text{eff}}$  is the flow stress of the material under the imposed conditions and  $\rho$  is the density. It is possible to estimate the flow stress of the densified Nb–Si or Mo–Si mixture from a constitutive equation, such as the Johnson–Cook equation [48]

$$\sigma = (\sigma_0 + B\epsilon^n) \left( 1 + C \log \frac{\dot{\epsilon}}{\dot{\epsilon}_0} \right) \left( 1 + \frac{T^*}{T_m^*} \right)^m \quad (5)$$

$\sigma_0$ ,  $B$ ,  $C$ ,  $m$  and  $n$  are parameters and  $T^*$  and  $T_m^*$  are normalized reference and melting temperatures. Ignoring work hardening and thermal softening, Eq. 5 is reduced to:

$$\sigma = \sigma_0 \left( 1 + C \log \frac{\dot{\epsilon}}{\dot{\epsilon}_0} \right) \quad (6)$$

It is possible to estimate the strain rate from the collapse velocity of the capsule containing the powder. It has been estimated to be equal to 800 m s<sup>-1</sup>, by Ferreira et al. [49]. Thus, the strain rate is ( $2r$  is the diameter of the capsule):

$$\dot{\epsilon} = \frac{v}{2r} = \frac{800}{10 \times 10^{-3}} \cong 0.8 \times 10^5 \text{ s}^{-1} \quad (7)$$

The compressive strength of Nb, under quasi-static conditions, is  $\approx 300$  MPa [50]; for Si, it is estimated to be 90 MPa. The value of  $C$ , the strain-rate sensitivity, can be estimated from data collected by Johnson and Cook [48]. From an average value for a number of materials ( $C = 1$ ), and applying Eq. 6, the flow stress can be estimated as:

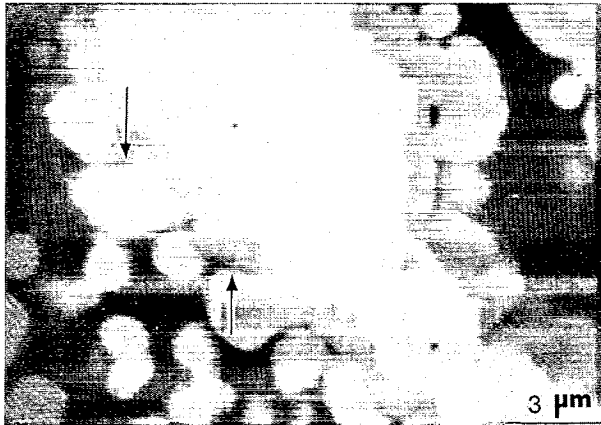
$$\sigma_{\text{eff}} = 800 \text{ MPa}$$

The application of Eq. 4 leads to the estimate of the deformation energy ( $\rho \cong 4.3 \times 10^3$  kg m<sup>-3</sup>)

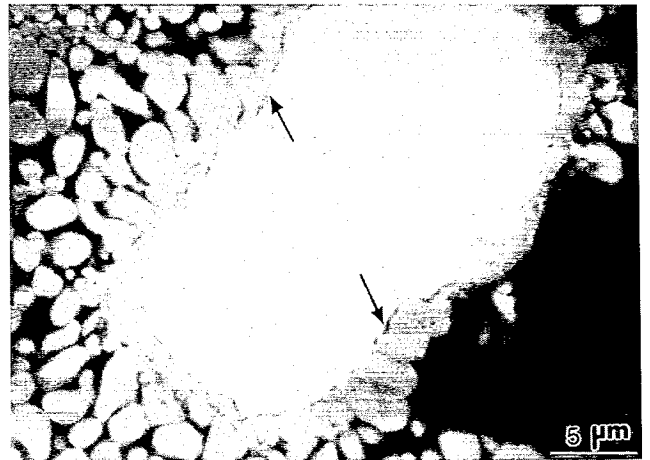
$$E_d = 120 \text{ J g}^{-1}$$

This value is quite low in comparison with the shock energy in experiments by Meyers et al. [27] to initiate the reaction based on experimental observations: 700–1200 J g<sup>-1</sup>. The Krueger–Vreeland threshold energy expression has the form:

$$E_{\text{th}} = E_s = \frac{1}{2} P (V_{00} - V) \quad (8)$$



(a)



(b)

Fig. 7. (a) Niobium and (b) molybdenum particles surrounded by reaction products.



where  $E_{th}$  and  $E_s$  are the threshold and shock energies (equal),  $P$  is the shock pressure, and  $V_{00}$  and  $V$  are the initial and shock specific volumes, respectively. The Krueger–Vreeland threshold energy includes, at the micro-mechanical level, the energy necessary to collapse the voids (geometrically-necessary plastic deformation), microkinetic energy (proposed by Nesterenko [51]) and a frictional energy. The various energetic terms are described by Meyers et al. [52]. The microkinetic energy represents, to a first approximation, the difference between the  $P$ – $V$  triangle and the “quasi-static” densification energy, which is reasonably well represented by the Carroll–Holt expression. Yu et al. [41] proposed a modified expression for the minimum energy which incorporates the plastic deformation energy. The total energy is the sum of the shock energy (which incorporates plastic deformation) and the deformation energy,  $E_d$ , due to non-shock processes:

$$E_t = E_s + E_d = \frac{1}{2}P(V_{00} - V) + \left(1 + C \log \frac{\dot{\epsilon}}{\dot{\epsilon}_0}\right) \epsilon_{eff} \quad (9)$$

The condition for initiation is, then:

$$E_t \geq E_{th}$$

The asymmetric experiments yielded shock energies (Eq. 8) of  $190 \text{ J g}^{-1}$  and  $300 \text{ J g}^{-1}$  for ammonit and RDX, respectively; the energy due to macroscopic plastic deformation ( $120 \text{ J g}^{-1}$ ). Applying Eq. 9:

$$(E_t)_{\text{ammonit}} = 310 \text{ J g}^{-1}$$

$$(E_t)_{\text{RDX}} = 420 \text{ J g}^{-1}$$

These values are still insufficient to initiate the reaction.

Localization of plastic deformation in narrow shear bands was observed in the system shock compressed with RDX (detonation velocity of  $6.2 \text{ km s}^{-1}$  and pressure of 6 GPa). Within the shear localization region high plastic strains are set up. Recent experiments by

Nesterenko et al. [42] revealed shear localization in Nb–Si powder mixtures subjected to compression in a cylindrical geometry (thick walled cylinder method). They were able to estimate the shear strains within the bands, which exceeded 10. Fig. 8 shows two such areas for Nb + 2Si and Mo + 2Si, respectively. The shear-band areas are characterized by fracturing of the Nb particles. The energy of deformation, for a shear strain of 10, ignoring thermal softening, is equal to  $1000 \text{ J g}^{-1}$ . This value is of the same order of magnitude as the threshold energy and can indeed be sufficient to trigger the reaction. Indeed, selected areas within the shear localization regions exhibited clear evidence of reaction; this is shown in Fig. 9. The reacted areas are marked by arrows A in Fig. 9(a). The deformed Nb particles and flaky splinters, produced by the intense plastic deformation, are surrounded by reacted material. The mechanism for reaction seems to be the same as that under shock compression, but the diameter of the spherules is considerably smaller:  $0.1\text{--}0.4 \text{ }\mu\text{m}$ , as seen in Fig. 9(b). The silicon in Fig. 9(a) shows spheroidal voids (marked by arrow B) and this is strongly suggestive of melting and resolidification.

#### 4. Conclusions

Shock compression (using an explosive with detonation velocity of  $7.4 \text{ km s}^{-1}$ ) of Nb–Si and Mo–Si elemental powder mixtures in cylindrical capsules yielded two regimes of pressure: a central Mach stem with a pressure of  $\approx 70 \text{ GPa}$ , and a peripheral area with  $P \approx 10 \text{ GPa}$ . The pressure was sufficient produce full reaction with complete melting. Although the experiments do not directly allow to establish whether the reaction is shock-assisted or shock-induced (completion after and during shock process, respectively) the sharp reacted–unreacted interface strongly suggests a shock-

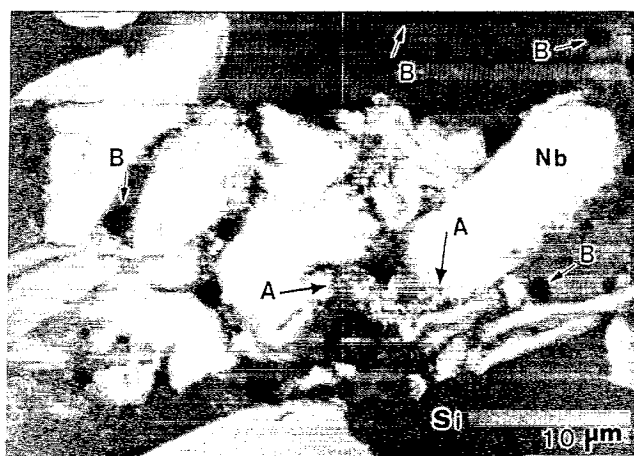


(a)

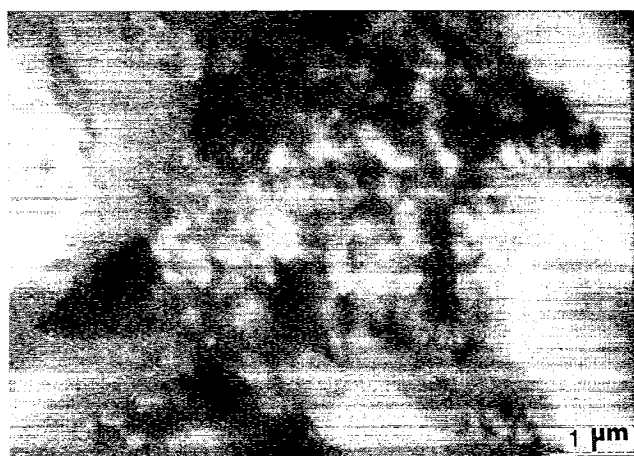


(b)

Fig. 8. Shear localization in (a) Nb + Si and (b) Mo + 2Si systems subjected to asymmetric compression.



(a)



(b)

Fig. 9. Reaction between Mo and Si in region subjected to intense shear localization: (a) overall view with spheroidal pores in Si (see arrows); (b) details of reaction products.

induced reaction; the peripheral region did not exhibit reaction. At the boundary between the two regions, a partially reacted region was observed, and the mechanism of reaction was by the formation of a liquid reacted Nb–Si or Mo–Si layer surrounding the solid Nb and Mo particles, respectively; this was followed by their spheroidization by interfacial energy minimization, solidification, and detachment from the interface. The mechanism is the same as that proposed by Meyers et al. [27]. It was demonstrated that intense localized shear deformation can trigger the exothermic reaction between Nb and Si, and Mo and Si particles at shock compression pressures below the threshold value for shock-induced reactions. It is proposed that plastic deformation provides the added driving energy for the reaction. Krueger and Vreeland [26] proposed that a threshold energy level exists for shock-induced (or shock-assisted) chemical reaction based on calculated homogeneous temperature being in excess of that required to initiate reactions in unshocked powder mixtures. Meyers et al. [28] provided a physical interpretation for this threshold energy by equating it to the energy required to form a melt pool of critical size; smaller melt pools would quench due to heat extraction by the surroundings whereas larger pool sizes would act as reaction initiation sites. This criterion has been modified to incorporate the plastic deformation energy as a component of the total energy. The results are in qualitative agreement with this modified criterion. Regions of intense shear localization were observed to initiate chemical reactions, in accordance with earlier observations by Bridgman [31–33], and Enikolopyan and co-workers [36–39]. Dremin and Breusov [29] emphasized the importance of shear strains in chemical processes during shock compression, and the current results are in full accordance with their proposal.

### Acknowledgements

This research was supported by the U.S. Army Research Office Contract DAAH04-93-G-0261, by the National Science Foundation Grant MSS-9021671, Office of Naval Research Contract N00014-94-1-1040, and by the Institute for Mechanics and Materials. The help provided by Y.J. Chen and M.S. Hsu is greatly acknowledged.

### References

- [1] Yu. N. Ryabinin, *Soviet Phys. Tech., Phys.*, 1 (1956) 2575.
- [2] D. Bankcroft, E.L. Peterson and S. Minshall, *J. Appl. Phys.*, 27 (1957) 291.
- [3] P.S. DeCarli, U.S. Patent No. 3, 238, 019, March 1, (1966).
- [4] P.S. DeCarli and J.C. Jamieson, *Science*, 133 (1961) 1821.
- [5] Y. Nomura, *Kagaku Kogyu*, 16 (1963) 123.
- [6] Y. Nomura, *J. Less-Common Metals*, 11 (1966) 378.
- [7] Y. Horiguchi, *J. Am. Ceram. Soc.*, 49 (1966) 519.
- [8] G.A. Adadurov, I.M. Barkalov, V.I. Goldanskii, A.N. Dremin, T.N. Ignatovich, A.M. Mikhailov, V.I. Talroze and P.A. Tampolskii, *Polymer Sci. USSR*, 7 (1965) 196.
- [9] S.S. Batsanov and A.A. Deribas, *Combustion, Explosion Shock Waves*, 1 (1965) 77.
- [10] R.A. Graham, B. Morosin, E.L. Venturini and M.J. Carr, *Annu. Rev. Mater. Sci.*, 16 (1986) 315.
- [11] Y. Horie, in J.R. Asay et al. (eds.), *Shock Waves in Condensed Matter—1983*, Elsevier, 1984, p. 369.
- [12] Y. Horie, R.A. Graham and I.K. Simonsen, *Mater. Lett.*, 3 (1985) 354.
- [13] Y. Horie and M.E. Kipp, *J. Appl. Phys.*, 63 (1988) 5718.
- [14] M.A. Lange and T.J. Ahrens, *J. Earth Plan. Sci. Lett.*, 77 (1986) 409.
- [15] R.A. Graham, *Solids Under High-Pressure Shock Compression*, Springer, New York, 1993.
- [16] Y. Horie and A.B. Sawaoka, *Shock Compression Chemistry of Materials*, KTK Scientific Publ., Japan, 1993.
- [17] S.S. Batsanov, *Effect of Explosions on Materials*, Springer, New York, 1994.
- [18] N.N. Thadhani, *Prog. Mater. Sci.*, 37 (1992) 117.



- [19] G. Duvall, Chairman, *Shock Compression Chemistry in Materials Synthesis and Processing*, National Materials Advisory Board, NMAB-414, WA, Natl. Acad. Press, 1984.
- [20] S.S. Batsanov, G.S. Doronin, S.V. Klochkov and A.I. Teut, *Combustion, Explosion Shock Waves*, 22 (1986) 765.
- [21] S.S. Batsanov, M.F. Gogulya, M.A. Bzazhnikov, E.V. Lazareva, G.S. Doronin, S.V. Klochkov, M.B. Banshikova, A.V. Fedorov and G.V. Simakov, *Sov. J. Chem. Phys.*, 10 (1991) 1699.
- [22] M.B. Boslough, *J. Chem. Phys.*, 92 (3) (1990) 1839.
- [23] L.H. Yu and M.A. Meyers, *J. Mater. Sci.*, 26 (1991) 601.
- [24] B.R. Krueger, A.M. Mutz and T. Vreeland, Jr., *J. Appl. Phys.*, 70 (10) (1991) 5362.
- [25] B.R. Krueger, A.M. Mutz and T. Vreeland, Jr., *Metall. Trans.*, 23A (1991) 55.
- [26] B.R. Krueger and T. Jr. Vreeland, in M.A. Meyers, L.E. Murr and K.P. Staudhammer (eds.), *Shock-Wave and High-Strain-Rate Phenomena in Materials*, Marcel Dekker, New York, 1992, 245.
- [27] K.S. Vecchio, L.H. Yu and M.A. Meyers, *Acta Metall. Mater.*, 42 (1994) 701.
- [28] M.A. Meyers, L.H. Yu and K.S. Vecchio, *Acta Metall. Mater.*, 42 (1994) 715.
- [29] A.N. Dremin and O.N. Breusov, *Russ. Chem. Rev.*, 37 (1968) 392.
- [30] P.W. Bridgman, *Phys. Rev.*, 48 (1935) 825.
- [31] P.W. Bridgman, *Proc. Am. Acad. Arts Sci.*, 71 (1937) 9.
- [32] P.W. Bridgman, *J. Chem. Phys.*, 15 (1947) 311. [33] P.W. Bridgman, *The Physics of High Pressure*, Bell, London, 1949.
- [34] L.F. Vereshchagin, E.v. Zubova and V.A. Shapochkin, *Pribori Tekhn. Esperim.*, 5 (1960) 89.
- [35] E. Teller, *J. Chem. Phys.*, 36 (1962) 901.
- [36] N.S. Enikolopyan, *Dokl. Akad. Nauk. SSSR*, 302 (1988) 630.
- [37] N.S. Enikolopyan, *Russ. J. Phys. Chem.*, 63 (1989) 1261.
- [38] N.S. Enikolopyan, A.A. Mkhitarian, A.S. Karagezyan and A.A. Khazardzhyan, *Dok. Akad. Nauk. SSSR*, 292 (1987) 887.
- [39] V.A. Zhorin, A.V. Nefed'ev, V.A. Linskii, Y.N. Novikov, R.A. Stukan, M.E. Volpin, V.I. Gold'anskii and N.S. Enikolopyan, *Dokl. Akad. Nauk. SSSR*, 256 (1981) 598.
- [40] M.A. Meyers, *Dynamic Behavior of Materials*, J. Wiley, New York, 1994, p. 640.
- [41] L.H. Yu, W. Nellis, M.A. Meyers and K.S. Vecchio, in S.C. Schmidt, J.W. Shaner, G.A. Samara and M. Ross (eds.), *Shock Compression of Condensed Matter-1993*, Am. Inst. Physics, 1994, p. 1291.
- [42] V.F. Nesterenko, M.A. Meyers, H.C. Chen and J.C. LaSalvia, *Appl. Phys. Lett.*, 65 (1994) 3069.
- [43] R. Prummer, *Explosivverdichtung Pulvriger Substanzen*, Springer, Berlin, 1982.
- [44] M.A. Meyers and S.L. Wang, *Acta Metall.*, 36 (1988) 925.
- [45] J. Reaugh, *J. Appl. Phys.*, 61 (3) (1987) 962.
- [46] N.N. Thadhani, *J. Appl. Phys.*, 76 (1994) 2129.
- [47] L.H. Yu and M.A. Meyers, in M.A. Meyers, L.E. Murr and K.P. Staudhammer (eds.), *Shock-Wave and High-Strain-Rate Phenomena in Materials*, M. Dekker, New York, 1992, p. 303.
- [48] G. Johnson and W. Cook, *Proc. 7th Int. Symp. on Ballistics*, Hague, Netherlands, 1983, p. 955.
- [49] A. Ferreira, M.A. Meyers, N.N. Thadhani, S.N. Chang and J.R. Kough, *Met. Trans.*, 22A (1991) 685.
- [50] H.E. Boyer and T.L. Gall (eds.), *Metals Handbook*, Desk Edition, ASM, 1985, 14.9, 14.10.
- [51] V.F. Nesterenko, *High-rate Deformation of Heterogeneous Materials*, Nauka, Novosibirsk, 1992, p. 31.
- [52] M.A. Meyers, S.S. Shang and K. Hokamoto, in A.B. Sawaoka (ed.), *Shock Waves in Materials Science*, Springer, Tokyo, 1993, p. 145.